Inter-Sensor Comparison of Satellite Ocean Color Products from GOCI and MODIS

Conference Paper · January 2013

9 authors, including:

Sherwin Ladner
United States Naval Research Laboratory
74 PUBLICATIONS **409** CITATIONS

SEE PROFILE

Igor Shulman
United States Naval Research Laboratory
68 PUBLICATIONS **1,320** CITATIONS

SEE PROFILE

Jason Keith Jolliff
United States Naval Research Laboratory
65 PUBLICATIONS **1,032** CITATIONS

SEE PROFILE

Some of the authors of this publication are also working on these related projects:

Project   Maritime Advanced Geospatial Intelligence Craft View project

Project   VIIRS val/cal View project

Inter-Sensor Comparison of Satellite Ocean Color Products from GOCI and MODIS

Ruhul Amin[1], Richard Gould[1], Sherwin Ladner[1], Igor Shulman[1], Jason Jolliff[1], Peter Sakalaukus[1], Adam Lawson[1], Paul Martinolich[2], and Robert Arnone[1]

[1]Naval Research Laboratory, Code 7331, Stennis Space Center, Mississippi 39529, USA
[2]Qinetic North America, c/o Naval Research Laboratory, Code 7331, Stennis Space Center, Mississippi 39529, USA

Corresponding author address: Ruhul Amin, Naval Research Laboratory, Code 7331, Stennis Space Center, Mississippi 39529, USA
E-mail: ruhul.amin@nrlssc.navy.mil

Abstract

The Geostationary Ocean Color Imager (GOCI) is the first geostationary ocean color satellite sensor that collects images every hour during the day. This high temporal frequency can lead to improved understanding of short time scale optical and bio-optical variability in the ocean surface. However, such study can be complicated by the imperfect atmospheric corrections particularly in turbid coastal waters. In this study we use the Red Band Difference (RBD) and the Fluorescence Line Height (FLH) algorithms, which have been found to be less sensitive to atmospheric corrections and CDOM absorption, to separate waters with high algal and non-algal particles from the GOCI imagery and monitor their movement. The Moderate Resolution Imaging Spectroradiometer (MODIS) imagery is used as the ground truth and good agreement is found between the two sensors. The dynamics of the turbid waters observed by GOCI is consistent with currents predicted by the Navy Coastal Ocean Model (NCOM).

1.   Introduction

The Geostationary Ocean Color Imager (GOCI) is one of the three payloads of the Korean Communication, Ocean and Meteorological Satellite (COMS) that was successfully launched in June 2010 from the Space Center in Kourou, French Guiana by Ariane 5 Launch Vehicle. GOCI is the world's first geostationary ocean color sensor designed with visible and near-infrared band that can measure radiance from the ocean surface. The advantage of GOCI is that it can obtain images every hour during the day which makes it possible to monitor ocean in near real time. GOCI covers $2,500 \times 2,500$ km square around Korean Peninsula centered at 36°N and 130°E with about 500 m pixel size and it is comprised of sixteen (4×4) slot images. It also has very high signal-to-noise ratio (over 1 thousand) which is necessary for detection of very weak variation of ocean signal. GOCI has six visible bands with band centered at 412 nm, 443 nm, 555 nm, 660 nm and 680 nm, and two near-infrared bands with band center at 745 nm and 865 nm. The life expectancy of GOCI mission is about seven years.

Polar-orbiting satellite sensors such as the Moderate Resolution Imaging Spectroradiometer (MODIS) and the MEdium Resolution Imaging Spectrometer (MERIS) have been widely used for ocean color studies. However, those sensors have limitations in monitoring dynamic variation such as daily or hourly variation of the ocean surface. These sensors typically collect data at about 1km resolution and 1 image per day in cloud-free periods. While these sensors provide an enormous advantage in terms of spatial coverage, cloud coverage is a serious restriction for these sensors. Daily revisit time is another limitation for these sensors particularly in optically complex coastal waters which frequently changes due to tide, wind-driven advection, resuspension, etc.

For these reasons, a geostationary sensor with high temporal frequency is ideal. Even though cost increases greatly for higher orbit geostationary platforms compare to polar-orbiting platforms and give a reduction in spatial resolution for the same optical system, high frequency satellite observations are critical to studying and quantifying biological and physical processes within the coastal ocean. Unlike polar-orbiting satellites which provide only one or two images of the same geographic area per day, GOCI collects images every hour from 00:00 GMT to 07:00 GMT (total eight images per day). This high frequency image acquisition makes it possible to study more detailed time-series analyses and movement of red tide, sediments, CDOM plume, predicting short term and long term biophysical phenomena, etc.

Although GOCI is the first geostationary ocean color sensor, geostationary platforms with the Spinning Enhanced Visible and InfraRed Image (SEVIRI) meteorological sensor has been used to map Suspended Particulate Matter (SPM) in turbid coastal waters Neukermans et al., (2009). GOCI also has been used to map turbidity around the coastal region of Korean Peninsula Choi et al., (2012) and Ryu et al., (2011). However, those studies used algorithms that may have been sensitive to atmospheric correction. In this study we use the Red Band Difference (RBD) and Fluorescence Line Height (FLH) algorithms which are less sensitive to atmospheric corrections and Colored Dissolved Organic Matter (CDOM) absorption unlike to the blue-green band ratio algorithms Amin et al., (2009a, 2009b).

The objective of this study is to test the feasibility of separating algal and non-algal component from the turbidity map using GOCI imagery and to determine whether high frequency dynamics can be detected. We also attempt to track the algal and non-

algal features using hourly GOCI imagery and assess their movement against the Navy Coastal Ocean Model (NCOM) predicted current. GOCI atmospherically corrected data is tested against MODIS data for validation then high frequency dynamic is presented. Our result suggest that (1) mapping of turbidity is feasible with FLH, (2) turbidity maps are well correlated with MODIS (3) high concentrations of algal and non-algal component separation is also possible and agreement between the two sensors are reasonable (4) dynamics of the turbid waters is in agreement with the current predictions by the NCOM model . Finally, conclusions are drawn regarding feasibility of turbidity mapping, algal and non-algal component separation. We qualitatively investigate daily variation in turbidity due to algal and non-algal particles in the coastal waters of Korean Peninsula.

2.   Materials and Methods

a. Satellite Data

We acquired all eight GOCI L1B data for April 5, 2011 and also corresponding MODIS data for the validation purpose. Considering the illumination and viewing geometry, we excluded first and last GOCI imagery from our analysis. GOCI L1B data was processed through the standard GOCI Data Processing System (GDPS) and level-2 data was generated. GDPS have the atmospheric correction algorithms, as the spectral shape matching method, the sun glint correction algorithm, and BRDF algorithm for bi-directional problems Han et al., (2010) and Ryu et al., (2012). GDPS is also capable of generating ocean color products such as chlorophyll concentration, suspended sediment, and CDOM. However, for this study we only used normalized water-leaving radiances

(nLw) in the red and near-infrared (NIR) regions since FLH and RBD requires radiance/reflectance in these bands. We also processed same GOCI L1B data in addition to MODIS data through NRL's Automated Processing System (APS) Martinolich et al., (2011). Note that the APS is still under development to make it compatible for GOCI data processing. Thus APS results are preliminary and currently under investigation.

b. The NCOM model

The NCOM model is a primitive-equation, 3D, hydrostatic model. It uses the Mellor-Yamada level 2.5 turbulence closure scheme, and the Smagorinsky formulation for horizontal mixing Martin, (2000). The model is set up at 3km horizontal resolution and 50 vertical layers around the Korean Peninsula. The model is initialized on 00Z, 1 April, 2011 with sea surface height, temperature, salinity and velocities data derived from the 1/8º horizontal resolution NCOM global model Rhodes et al., (2002) and Barron et al., (2006) for 00Z, 1 April of 2011. The model is forced with surface fluxes from the Navy Global Atmospheric Prediction System (NOGAPS) Rosmond et al., (2002). Open boundary conditions for the NCOM model are derived from the NCOM global model. Tidal forcing is introduced by using tidal sea surface height and velocities at the model open boundaries from the Oregon State University (OSU) tidal model Egbert and Erofeeva, (2003). Eight tidal constituents (M2, S2, N2, K2, K1, O1, P1 and Q1) are used. For the assimilation of physical observations (temperature and salinity), the NCOM ICON model uses the Navy Coupled Ocean Data Assimilation (NCODA) system Cummings, (2005), and Cummings et al, (2009). The NCODA is a fully 3D multivariate optimum interpolation system. Assimilation of temperature and salinity data is

performed every 12 hours (assimilation cycle). The NCODA assimilates satellite altimeter observations, satellite surface temperature, as well as available in-situ vertical temperature and salinity profiles from XBTs, ARGO floats, moored buoys and gliders from the Global Ocean Data Assimilation Experiment (GODAE) data set. The description of the data sets, processing and quality control procedures are described in Cummings, (2005) and Cummings et al., (2009). Results of glider, ship and satellite data assimilation into the NCOM model for the Monterey Bay area are described in Shulman et al., (2009, 2011).

c. Algorithms

The Red Band Difference (RBD) algorithm was developed by taking advantage of the chlorophyll fluorescence emission centered on 685 nm Amin et al., (2009a). Since there is nothing else in the water that fluoresces in the red region, the RBD easily identifies chlorophyll rich regions from false chlorophyll-like features from CDOM plumes, sediment plumes, and bottom reflectance. The RBD algorithm is expressed as follows:

$$RBD = nLw(\lambda_2) - nLw(\lambda_1) \tag{1}$$

where $nLw(\lambda)$ is the normalized water-leaving radiance which is defined as the upwelling radiance just above the sea surface, in the absence of an atmosphere, and with sun directly overhead. The λ_1 is band 13 (667 nm) for MODIS and band 5 (660 nm) for GOCI while the λ_2 is band 14 (678 nm) for MODIS and band 6 (680 nm) for GOCI. The RBD approach has been used to detect algal blooms particularly dinoflagellates throughout world using MODIS and MERIS imagery Amin et al., (2009c). In this study,

the RBD approach is applied to GOCI imagery for the first time to detect high chlorophyll regions. To detect sediment rich water, we used FLH which is estimates using nLw at GOCI bands 5 (660 nm), 6 (680 nm) and 7 (745 nm).

3. Results and Discussion

Phytoplankton blooms develop over the course of a few days to a week and the complete dynamics of the blooms are not captured by individual Polar-orbiting satellite sensors. The physiology of phytoplankton cells (chlorophyll content, nutrient uptake, etc.) varies on diel cycles, and this has a significant impact on their growth rate and hence primary production Furnas, (1990). Therefore, multiple observations per day over several days would permit more robust satellite based estimates of primary production. However, for such estimation, we need more reliable atmospheric correction particularly for the coastal ocean. In coastal waters, the standard NASA NIR atmospheric correction Gordon and Wang, (1994) often fails due to higher turbidity and consequently significant higher radiance contributions in the NIR bands. Since the water-leaving radiance at NIR can no longer be considered negligible for the use of atmospheric correction for turbid waters Amin et al., (2009b) and Siegel et al., (2000), negative readings may result in the blue-green bands due to the over-correction of the atmosphere Hu et al., (2000). Algorithm that uses blue-green bands O'Reilly et al., (2000), Gordon et al., (1983) and Carder et al., (1999), have been found to perform poorly in coastal waters due to increased absorption of CDOM, increased particle scattering, inaccurate atmospheric correction and shallow bottom reflectance. Since atmospheric correction still remains a challenge in turbid waters, in this study we use algorithm that are less sensitive to atmospheric corrections.

MODIS Aqua chlorophyll image for April 5, 2011 over the Korean Peninsula is shown in Fig. 1a. Since chlorophyll is retrieve using blue-green bands, it often fails in coastal water and usually over estimate chlorophyll concentrations. In Fig. 1a, it can be seen that chlorophyll concentration is high in the coastal region particularly western and southern region. However, corresponding FLH images in Fig. 1b shows somewhat different features. Note that FLH uses red and NIR band where water absorption is significantly higher compare to the blue-green region. Thus FLH only sees first few meters of the surface waters which may contribute a little to the discrepancies between the two images but most of the discrepancies are probably from imperfect atmospheric correction, CDOM absorptions and bottom reflectance. Even though FLH is less sensitive to atmospheric correction and CDOM absorption, it breaks down in highly scattering waters, where high red peak values in the reflectance are primarily due to contributions from elastic scattering modulated by chlorophyll absorption rather than the fluorescence, thus falsely indicating possible chlorophyll rich areas. In contrast, the RBD technique is found to easily differentiate between the two effects, giving positive values under true bloom conditions and negative values in highly scattering waters. However, RBD approach is for high chlorophyll concentration (>1 mg/m^3) waters and it depends on chlorophyll fluorescence quantum yield and the backscattering properties of the particles in the water Amin et al., (2009a). Fig. 1c shows the corresponding MODIS RBD image where sediment rich area detected by FLH disappears as expected and only true chlorophyll rich area can be seen. This result is consistent with our previous study based on the west coast of Florida Amin et al., (2009a). The RBD and FLH algorithms have been validated for the MODIS sensor thus we use MODIS RBD and FLH image as the

ground truth to validate GOCI FLH and RBD images. Fig.1d and Fig. 1e shows GOCI

FLH and RBD images respectively that was acquired on April 5, 2011 at 04:16 GMT

about 16 min after MODIS acquisition. The data for these two images were processed

using the standard GOCI data processing system, GDPS. It can be seen clearly that

MODIS and GOCI FLH images detects nearly identical features, so is the RBD images.

This is probably due to the fact that these two algorithms are less sensitive to atmospheric

correction uncertainties and CDOM absorptions. Fig. 1f shows the APS processed RBD

image which agrees fairly well with the GDPS processed RBD image (Fig. 1e) both

showing similar biological features in the south eastern Korean coast. Since APS is still

under modification for GOCI data processing, it is too early to compare APS and GDPS

results quantitatively. However, in our preliminary comparison we noticed that GDPS

results agree better with MODIS results as of now. Although APS flags seems to work

relatively well while GDPS flags over removes pixels particularly turbid coastal pixels.

APS results are expected to improve over next few months which will allow a more

quantitative comparison between the two processing systems.

Fig. 2a shows MODIS SST image for April 5, 2011 while Fig. 2b shows

corresponding NCOM predicted SST and current. Even though NCOM model has not

been validated in the Korean Peninsula, it has been validated in other places such as the

Monterey Bay, California Shulman et al., (2009, 2011). It can be seen clearly in Fig. 2

that the agreement between satellite measured SST (Fig. 2a) and NCOM modeled SST

(Fig. 2b) is very reasonable. This suggests that the NCOM model is capable of predicting

reasonable SST and perhaps current data as well for the Korean Peninsula.

Western coast of Korea particularly around urban estuary, Kyunggi Bay, undergoes coastal erosion and geomorphologic changes near the tidal flats Kim et al., (2009). This sedimentary environment is influenced by the inland river systems and by the circulation of seawater due to tidal cycles Lee et al. (1998), Woo et al., (1998), Woo and Je, (2002). Kyunggi Bay is a shallow (<40 m) semi-enclosed region located on the eastern part of the Yellow Sea Kim et al., (2009). This area has large tidal range (4-8 m), strong tidal currents (1 – 2 m/s) and a large sediment supply (12.42×10^6 t/year) provided by the Han River Kim and Lim, (2009).

SPM plays a major role in ocean health particularly in coastal waters. In-situ measurement have shown that SPM can vary by a factor of two or more during the day due to horizontal advection and/or vertical resuspension forced by tides or wind events Eisma and Irion, (1988) and Thompson et al., (2011). Study of the temporal variations of SPM concentration on the sea surface is important to understand the erosion or sedimentation pattern in coastal regions, especially in the environment of semidiurnal tides Torres and Morelock, (2002) and Zhang et al., (2010). Temporal frequency afforded by GOCI makes it possible to study hourly temporal variation in the water surface.

GOCI FLH images are shown in Fig. 3 where the area with warm color indicates highly turbid region while the cool color indicates low turbid regions. Lands, clouds and invalid pixels are shown in white. Inset of each subfigure is the corresponding current map predicted by the NCOM model. According to NCOM model, current flows towards offshore waters in the Kyunggi Bay around 01:00 GMT (inset of Fig. 3a). Then it slowly reverses direction and start flowing towards the coast (inset of Fig. 3b to Fig. 3f). Similar

pattern can be seen in the FLH images as well where FLH image acquired around 01:16 GMT (Fig. 3a) has highest spatial extent of the SPM. SPM spatial extent gradually decreases as current rushes toward the coast. SPM spatial extent is lowest at 06:16 GMT (Fig. 3f) as expected from the NCOM current map (inset of Fig. 3f). This suggests that the SPM movement in this region is due to strong tidal forces. On the other hand, current is somewhat weaker in the southeastern part of Korean Peninsula as can been seen in Fig. 2b. Perhaps the relatively weak current may have allowed biological growth in this part of Korean Peninsula. Like the sediments, the biological component also follows the current (not shown).

4.   Conclusion

We show that the temporal frequency afforded by the GOCI sensor can be used effectively to detect and monitor the temporal dynamics of the turbidity due to algal and non-algal particles in the waters. We successfully separate the regions with high algal and non-algal particles from GOCI and validate the results with MODIS imagery. Good agreement between GOCI and MODIS also suggest that the GOCI sensor is capable of producing quality ocean color products. Sediment movement shown by hourly GOCI FLH images agrees well with the dynamics predicted by the NCOM model. However, further study with in-situ data is necessary to refine the results.

References

G. Neukermans, K. Ruddick, E. Bernard, D. Ramon, B. Nechad, and P.-Y Deschamps, "Mapping total suspended matter from geostationary satellites: A feasibility study with SEVIRI in the Southern North Sea," Optics Express. 17, 14,029-14,052 (2009).

J. K. Choi, Y. J. Park, J. H. Ahn, H. S. Lim, J. Eom, and J. H. Ryu, "GOCI, the world's first geostationary ocean color observation satellite, for the monitoring of temporal variability in coastal water turbidity," J. Geophys. Res., Vol. 117, c09004, doi: 10.1029/2012JC008046 (2012).

J. H. Ryu, J. K. Choi, J. Eom, and J. H. Ahn, "Temporal variation in Korean coastal waters using Geostationary Ocean Color Imager," J. Coastal Res. Spec. Issue, 64, 1731-1735 (2011).

R. Amin, J. Zhou, A. Gilerson, B. Gross, F. Moshary and S. Ahmed, "Novel Optical Techniques for Detecting and Classifying Toxic Dinoflagellate Karenia brevis Blooms Using Satellite Imagery*," Optics Express Vol. 17, Iss.* 11, pp. 9126-9144 (2009a).

R. Amin, A. Gilerson, J. Zhou, B. Gross, F. Moshary, and S. Ahmed, " Impacts of atmospheric corrections on algal bloom detection techniques," 89th AMS Annual Meeting, Phoenix, Arizona, 11-15 Jan, (2009b).

H. J. Han, J. H. Ryu, and Y. H. Ahn, "Development of Geostationary Ocean Color Imager (GOCI) Data Processing System (GDPS)," Korean Journal of Remote Sensing, 26(2), 239-249 (2010).

J. H. Ryu, H. J. Han, S. Cho, Y. J. Park, and Y. H. Ahn, "Overview of Geostationary Ocean Color Imager (GOCI) and GOCI Data processing System (GDPS)," Ocean Sci, J., 47(3), 223-233 (2012).

P. Martinolich, and T. Scardino, "Automated Processing System User's Guide Version 4.2," http://www7333.nrlssc.navy.mil/docs/aps_v4.2/html/user/aps_chunk/index.xhtml, NRL, Washington, D.C., (2011)

P. J. Martin, "Description of the Navy Coastal Ocean Model version 1.0," Rep. NRL/FR/732-00—9962, Nav. Res. Lab., Stennis Space Center, Miss. (2000).

R. C. Rhodes, O. M. Smedstad, S. L. Cross, A. B. Kara, "Navy real-time global modeling systems," Oceanography, 15(1), 29–43 (2002).

C. N. Barron, A. B. Kara, P. J. Martin, R. C. Rhodes, and L. F. Smedstad, "Formulation, implementation and examination of vertical coordinate choices in the global Navy Coastal Ocean Model (NCOM)," Ocean Model., 11(3–4), 347–375, doi:10.1016/j.ocemod.2005.01.004 (2006).

T. E. Rosmond, J. Teixeira, M. Peng, T. F. Hogan, and R. Pauley, "Navy Operational Global Atmospheric Prediction System (NOGAPS): Forcing for ocean models," Oceanography, 15, 99-108 (2002).

G. D. Egbert, and S. Y. Erofeeva, "Efficient inverse modeling of barotropic ocean tides," J. Atmos. Oceanic Technol., 19, 183-204 (2003).

J. Cummings, L. Bertino, P. Brasseur, I. Fukumori, M. Kamachi, M. J. Martin, K. Mogensen, P. Oke, C. E. Testud, J. Verron, and A. Weaver, "Ocean Data Assimilation Systems for GODAE," Oceanography, 22, 3, 96-109 (2009).

J. Cummings, "Operational multivariate ocean data assimilation," Q. J. R. Meteorol. Soc., 131, 3583–3604, doi:10.1256/qj.05.105 (2005).

I. Shulman, C. Rowley, S. Anderson, S. DeRada, J. Kindle, P. Martin, J. Doyle, J. Cummings, S. Ramp, F. Chavez, D. Fratantoni, and R. Davis, "Impact of glider data assimilation on the Monterey Bay model," Deep Sea Res. Part II, 56, 128–138 (2009).

I. Shulman, M. A. Moline, B. Penta, S. Anderson, M. Oliver, and S. H. D. Haddock, "Observed and modeled bio-optical, bioluminescent, and physical properties during a coastal upwelling event in Monterey Bay, California," J. Goephys. Res., 116, C01018, doi:10.1029/2010JC006525 (2011).

R. Amin, A. Gilerson, B. Gross, F. Moshary, and S. Ahmed, "MODIS and MERIS Detection of Dinoflagellates Blooms using the RBD Technique," SPIE Europe Remote Sensing, Berlin, Germany, August 31- September 3, (2009c).

M. J. Furnas, "In situ growth rates of marine phytoplankton: approaches to measurement, community and species growth rates," J. Plankton Res., 12, 1117-1151, doi:10.1093/plankt/12.6.1117 (1990).

H. R. Gordon, and M. Wang, "Retrieval of water-leaving radiance and aerosol optical thickness over the oceans with SeaWiFS: a preliminary algorithm," Appl. Opt. 33, 443-452 (1994).

D. A. Siegel, M. Wang, S. Maritorena, and W. Robinson, "Atmospheric correction of satellite ocean color imagery: the black pixel assumption," Appl. Opt. 39(21), 3582-3591 (2000).

C. Hu, K. L. Carder, and F. E. Muller-Karger, "Atmospheric correction of SeaWiFS imagery over turbid coastal waters: a practical method," Remote Sens. Environ. 74(2), 195-206 (2000).

J. E. O'Reilly, S. Maritorena, D. Siegel, M. C. O'Brien, D. Toole, B. G., Mitchell, et al., "Ocean color chlorophyll a algorithms for SeaWiFS, OC2, and OC4: version 4," In: Hooker, S. B. & Firestone, E. R. (Eds.), SeaWiFS Postlaunch Calibration and Validation Analyses, Part 3 SeaWiFS Postlaunch Technical Report Series, (pp. 9-23) Greenbelt, Maryland: NASA, Goddard Space Flight Center (2000).

H. R. Gordon, D. K. Clark, J. W. Brown, O. B. Brown, R. H. Evans, W. W. Broenkow, "Phytoplankton pigment concentrations in the Middle Atlantic Bight: comparison of ship determinations and CZCS estimates," Appl. Opt. 22, 20-36, (1983).

K. L. Carder, F. R. Chen, Z. P. Lee, S. K. Hawes, D. Kamykowski, "Semi-analytic moderate-resolution imaging spectrometer algorithms for chlorophyll a and absorption with bio-optical domains based on nitrate-depletion temperatures," J. Geophy. Res. 104, 5403-5422, (1999).

C. S. Kim, H. S. Lim, J. A. Kim, and S. J. Kim, "Residual flow and its implication to macro-tidal flats in Kyunggi Bay estuary of Korea," J. Coastal Res., Spec. Issue 56, 976-980 (2009).

H. J. Lee, U. H. Kim, and Y. S. Chu, "Sedimentology of tidal flats on the west coast, Korea," Ocean Res., 20(2), 153-165 (1998).

H. J. Woo, S. K. Chang, and Y.S. Chu, "Recent foraminifera and surface sediments in tidal flats of the west coast of Korea," Ocean Res., 20(2), 63-72 (1998).

H. J. Woo and J. G. Je, "Changes of sedimentary environments in the southern tidal flat of Kanghwa island," (Korean ed.). Ocean and Polar Res., 24(4), 331-343 (2002).

C. S. Kim and H. S. Lim, "Sediment dispersal and deposition due to sand mining in the coastal waters of Korea, Cont. Shelf Res., 29(1), 194-204, doi:10.1016/j.csr.2008.01.017 (2009).

D. Eisma, and G. Irion, "Suspended matter and sediment transport," In W. Salomons, B. I. Bayne, E. K. Duursma, and U. Forstner (Eds.), Pollution of the North Sea: An assessment (pp. 20-33). Berlin: Springer (1988).

C. E. L. Thompson, F. Couceiro, G. R. Fones, R. Helsby, C. L. Amos, K. Black et al., "In situ flume measurements of resuspension in the North Sea," Estuarine Coastal and Shelf Science, 94, 77-88 (2011).

J. L. Torres, and J. Morelock, "Effect of terrigenous sediment influx on coral cover and linear extension rates of three Caribbean massive coral species," Caribbean Journal of Science, 38(3-4), 222-229 (2002).

M. Zhang, J. Tang, Q. Dong, Q. Song, and J. Ding, "Retrieval of total suspended matter concentration in the Yellow and East China Seas from MODIS imagery," Remote Sens. Environ., 114, 392-403 (2010).
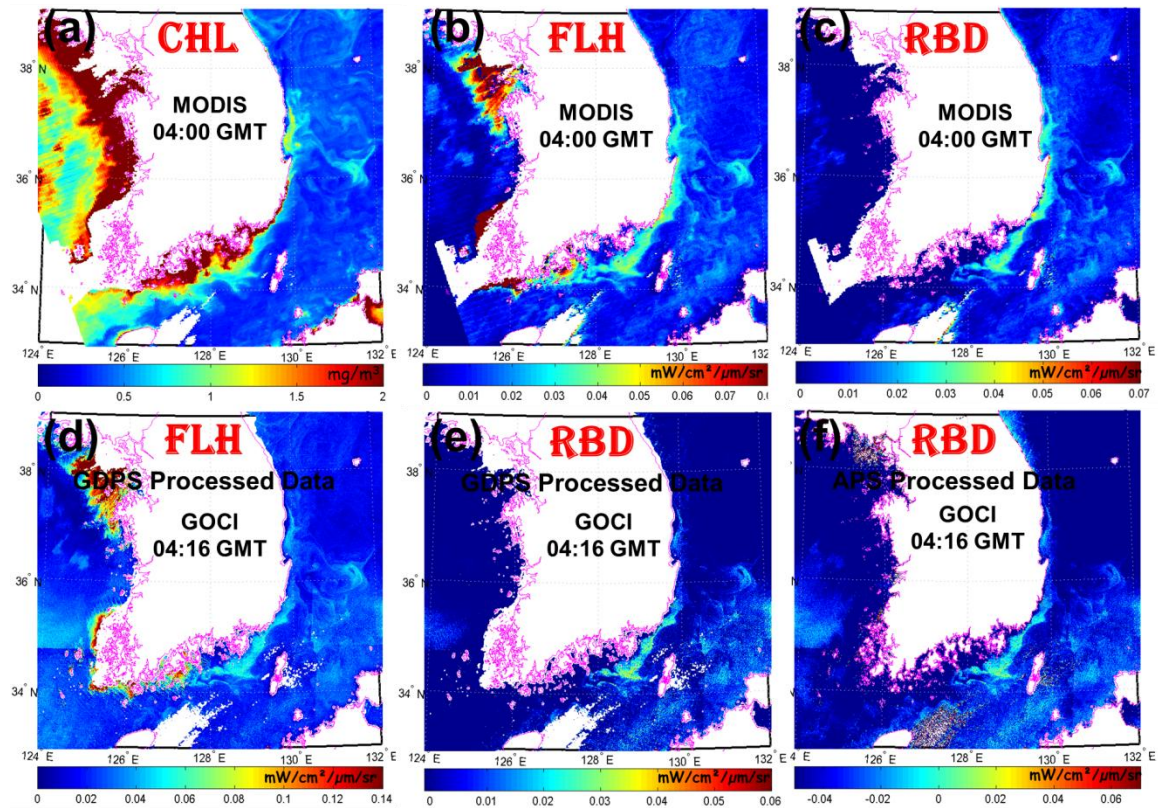
List of Figures

FIG. 1. Top panel showing MODIS ocean color products from April 5, 2011 acquired at 04:00 GMT: (a) Chlorophyll image, (b) FLH image, and (c) RBD image. Bottom panel showing GOCI image for April 5, 2011 acquired at 04:16 GMT: (d) GOCI FLH (data processed with GDPS), (e) GOCI RBD (data processed with GDPS), and (f) GOCI RBD (data processed with APS).

FIG. 2. (a) MODIS SST image for the April 5, 2011 and (b) corresponding NCOM modeled SST with current. Good agreement between the measured and modeled SST suggest that the NCOM model is capable of predicting good SST products and perhaps current products as well.

FIG. 3. FLH images of GOCI around Kyunggi Bay acquired at about (a) 01:16 GMT, (b) 02:16 GMT, (c) 03:16 GMT, (d) 04:16 GMT, (e) 05:16 GMT, and (f) 06:16 GMT on April 5, 2011. Inset is the corresponding current map predicted by the NCOM model.

FIG. 1. Top panel showing MODIS ocean color products from April 5, 2011 acquired at 04:00 GMT: (a) Chlorophyll image, (b) FLH image, and (c) RBD image. Bottom panel showing GOCI image for April 5, 2011 acquired at 04:16 GMT: (d) GOCI FLH (data processed with GDPS), (e) GOCI RBD (data processed with GDPS), and (f) GOCI RBD (data processed with APS).
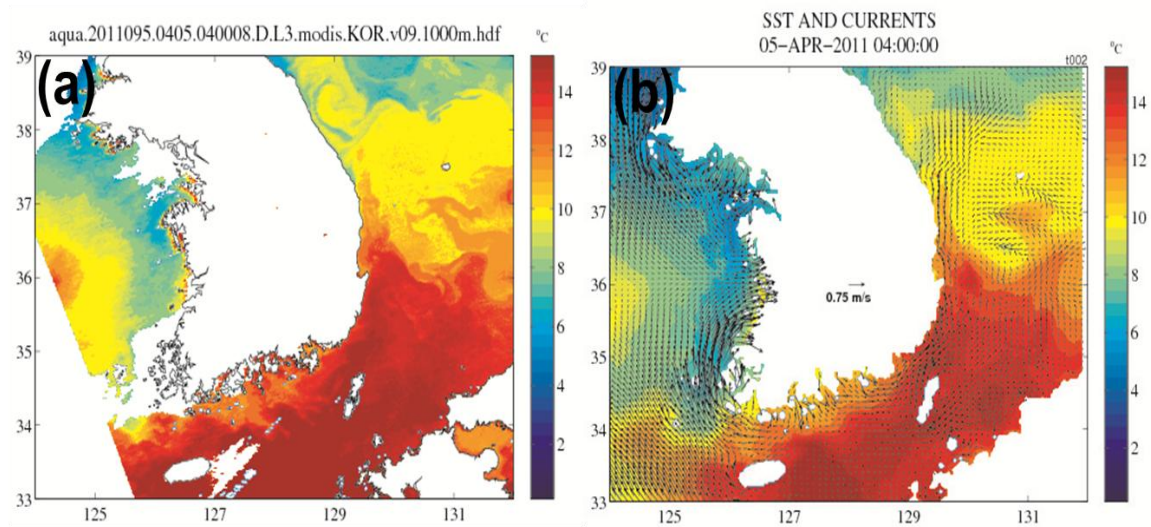
FIG. 2. (a) MODIS SST image for the April 5, 2011 and (b) corresponding NCOM modeled SST with current. Good agreement between the measured and modeled SST suggest that the NCOM model is capable of predicting good SST products and perhaps current products as well.
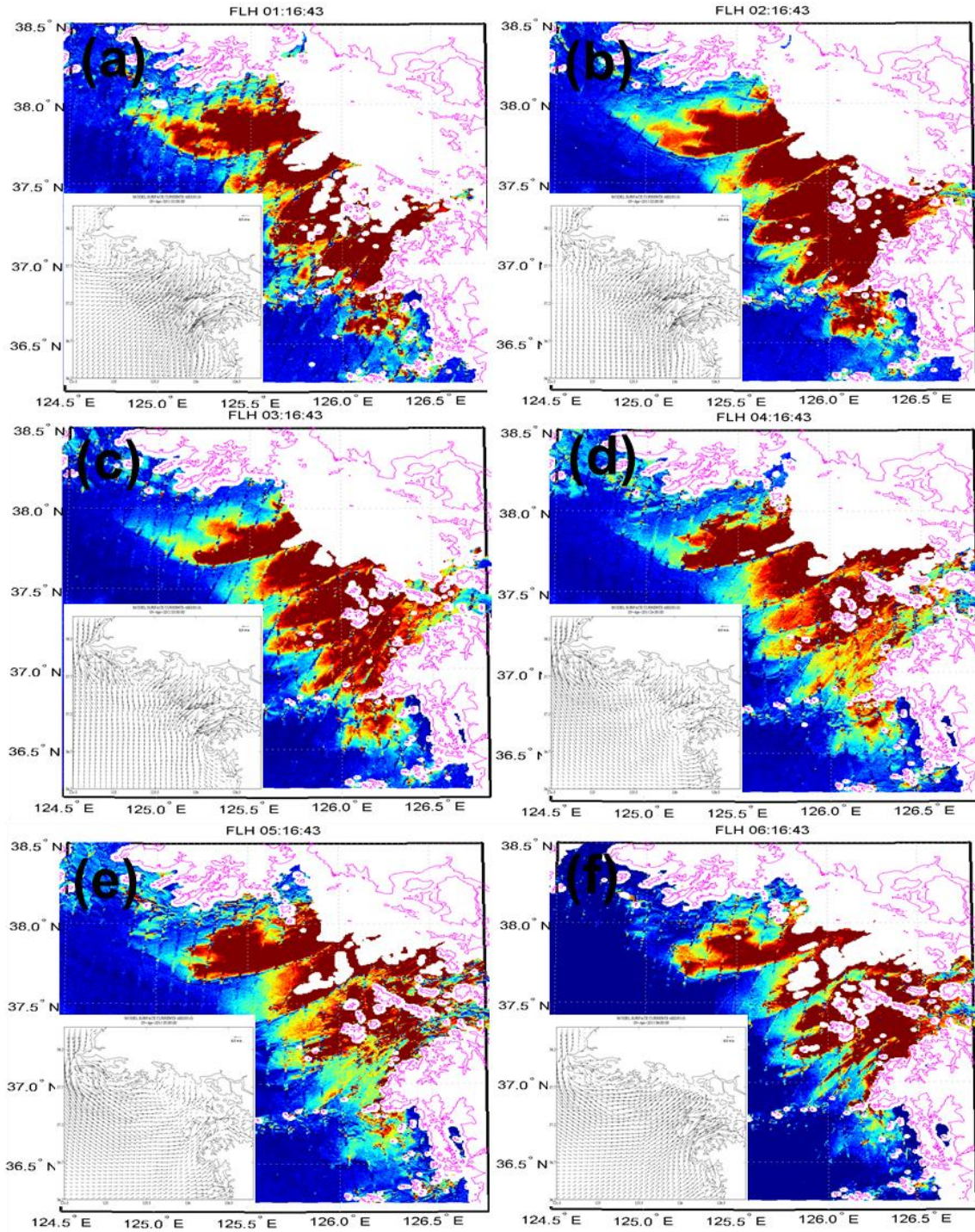
FIG. 3. FLH images of GOCI around Kyunggi Bay acquired at about (a) 01:16 GMT, (b) 02:16 GMT, (c) 03:16 GMT, (d) 04:16 GMT, (e) 05:16 GMT, and (f) 06:16 GMT on April 5, 2011. Inset is the corresponding current map predicted by the NCOM model.